1. This study uses Lagrangian particle tracking and Markov Chains to study the accumulation dynamics of water or passive/conservative mass in the PRE and connectivity among its subregions. Convergence and fronts were identified as major factors for high accumulation probability. The study is based on a validated model as the authors stated, yet more details on the model set up should be provided, particularly the sensitivity runs on modifying tide and river discharges. The identified seasonal accumulation dynamics in different subregions and their connectivity are interesting, yet more implications on the ecosystem in the PRE can be discussed. For example, based on the sensitivity run of reducing river discharge, should we worry about more pollutants will be accumulated in some regions in dry years? I also suggest the authors to carefully check the grammar and revise their writings to improve the clarity and readability of this manuscript. In addition, I am not familiar with the calculation of Markov Chains and I except other reviewers and the topic editors would have better judgements. Please find specific comments below.

Response: Thanks for reviewer's perceptive suggestions and comments, which are useful for us to improve our work. We responded to your concerns separately as below:

The study is based on a validated model as the authors stated, yet more details on the model set up should be provided, particularly the sensitivity runs on modifying tide and river discharges.

Response: Thanks for reviews' reminder. Our PRE model is developed using Regional Ocean Model System (ROMs) (Shchepetkin & McWilliams, 2005). The model region covers estuary and adjacent shelf between 112.3°E-115.68°E and 20.89°N-23.13°N (Figure R9). We adopt an orthogonal grid and the resolution increases from ~1km over shelf to ~200 m inside the estuary. In vertical direction, we use the terrain-following s-ordinate (Song & Haidvogel, 1994) to discretize the water column into 30 levels. The monthly averaged river discharge data is obtained from Ministry of Water Resources of China. During summer and winter, the river discharge is approximately 30000 m^3/s and 10000 m^3/s, respectively. Wind forcing, heat flux, and precipitation are obtained from the ERA5 atmospheric reanalysis data by European Centre for Medium-Range Weather Forecasts (ECMWF), and they are used to force ocean circulation through the implementation of the bulk computation algorithm (Fairall, Bradley, Hare, Grachev, & Edson, 2003). The shelf current is obtained from a coarser model (Deng et al., 2022), which can cover the North South China Sea and provide the information of barotropic and baroclinic velocities, temperature, salinity, sea level along the boundaries of PRE model. Turbulent and diffusion are determined by Mellor-Yamada 2.5 turbulence-closure module (Mellor & Yamada, 1982). Eight major tidal harmonic constants (M_2, S_2, K_2, N_2, K_1, O_1, P_1, Q_1) as well as the M_4 obtained from Zu, Gan, and Erofeeva (2008) are included to calculated the tidal induced current and elevation along the boundaries.

To test the influences of tide current and river discharge on the accumulation dynamics, two sensitivity tests were carried out. One is by removing the tide, i.e. not considering the tidal induced current and elevation along the open boundary conditions, the other one is by reducing the river discharge to 20% of the control run.

In the sensitivity tests, the experiments involve the removal of tide and a reduction of river discharge to 20%.

Above information will be integrated in Line 94-109 in the revised manuscript.

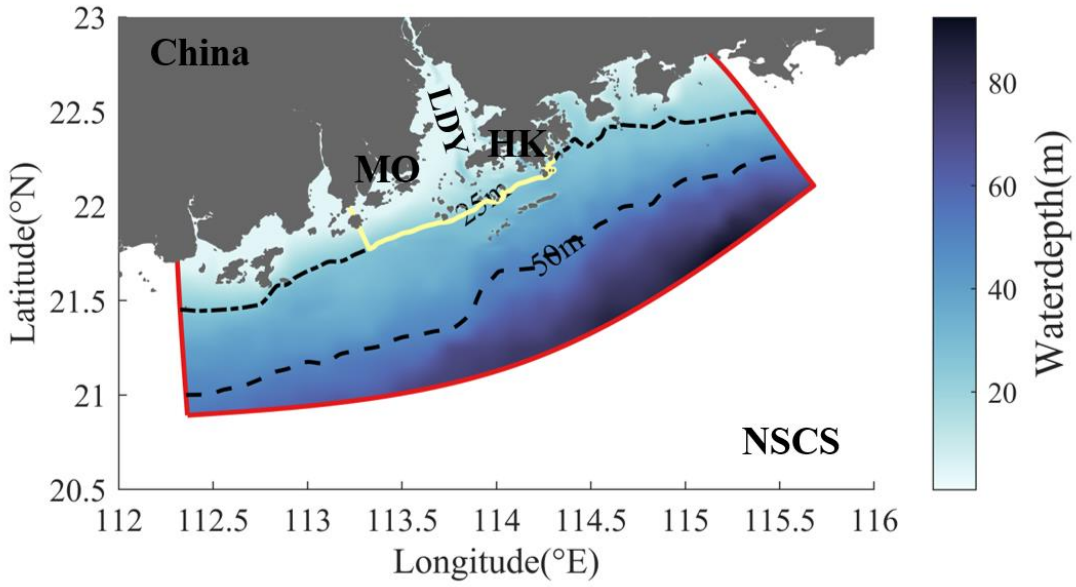

Figure R1. The bathymetry of study area. The black dotted and dashed lines represent the isobath of 25 m and 50 m. The yellow line defines the seaside boundary of the PRE. LDY, MO, HK and NSCS represent Lingdingyang, Macau, Hong Kong and northern South China Sea, respectively. The red line represents the model boundary.

The identified seasonal accumulation dynamics in different subregions and their connectivity are interesting, yet more implications on the ecosystem in the PRE can be discussed. For example, based on the sensitivity run of reducing river discharge, should we worry about more pollutants will be accumulated in some regions in dry years?

Response: Based on our sensitivity run, we noticed that the accumulations increased in UPPER and northern part of WEST region due to the reduction of river discharge. Similar results were found in the study of X. Zhang et al. (2013), the concentration of particle organic carbon and suspended solid in above mentioned regions in 2010 was much higher than that in 2011 during summertime, while the river discharges in 2010 was only half of the amount in 2011 during that time periods. Therefore, we thought it is possible that more pollutants will be accumulated in some regions in dry years.

I also suggest the authors to carefully check the grammar and revise their writings to improve the clarity and readability of this manuscript.

The grammar and the writing were improved in the revised manuscript.

2. Title: suggest revising it to specifically indicate that this study is about the accumulation dynamics of water (or passive material). Add 'a' before 'Lagrangian Perspective'.
   Response: Thanks a lot. The titles changes into 'Exploring Water Accumulation Dynamics in the Pearl River Estuary from a Lagrangian Perspective' in the revised manuscript.

3. Abstract and Conclusion need to be more concise. These long paragraphs will distract readers from the main takeaways. It is also necessary to mention that results in this study are based on a model with climatological forcings and not specific to a certain year that may have large variations in the hydrodynamics.
   Response: Thanks for reviewers' suggestions. The abstract and conclusion are compressed in the revised manuscript and the study is based on a climatological forcing model are mentioned in the manuscript Line 102-104 and Line 118-121.

   Line 102-104: "The shelf current was obtained from a coarser model with good validation that can cover the North-South China Sea and provide information on the barotropic and baroclinic velocities, temperature, salinity, and sea level along the boundaries of the PRE (Deng et al., 2022)."

   Line 118-121: "This model, primarily based on climatological data, was carefully verified using satellite remote sensing and long-term observations to ensure an accurate representation of the hydrodynamic properties (Fig. S2). Generally, the model captures the seasonal features of circulation in this region and has been used in previous studies (Cai, Liu, Liu, & Gan, 2022; Chu et al., 2022b; L. Cui, Liu, Chen, & Cai, 2024)."

   Abstract: Water accumulation is essential for understanding estuarine mass distribution and ecosystem management. In this study, we examined the water accumulation dynamics in the Pearl River Estuary (PRE) from a Lagrangian perspective. Generally, there is a notable negative correlation between the horizontal velocity divergence ($\nabla_h \vec{V}_h$) and the accumulation probability. Influenced by density fronts and velocity convergence, we observed significant bottom-layer accumulation of particles in the western estuary and Hong Kong waters during summer, whereas the accumulation moved landward in winter. Sub-regions with distinct accumulation patterns and interconnections were identified and combined with the trajectories. In summer, the western estuary and Macau waters have a substantial net negative $\nabla_h \vec{V}_h$ and strong density fronts are major accumulation targets, which

attract particles from the whole estuary. Conversely, the eastern estuary and Hong Kong waters exhibit significant westward motion, influencing the western side. In winter, particles are more likely to accumulate in their original locations. The upper estuary becomes a major accumulation area because of the obstructive density front, and decreased river discharges. The tidal currents and river discharges mainly control water accumulation in the estuary by changing the mixing or current intensity. The weakening of tidal currents and river discharges induced the intensified bottom intrusion and the landward movement of accumulation.

Conclusion: In this study, the Lagrangian method and Markov Chains were applied to illustrate the accumulation trends in different PRE regions during typical monsoon seasons.
The accumulation probabilities were obtained from the Markov Chains. Generally, surface offshore transport is always quicker than that at the bottom owing to the strong offshore current and river discharge, which are related to the relatively small accumulation at the surface layer. At the bottom, a high accumulation of water appears in the lower estuary in summer and moves shoreward in winter owing to the reduced river discharge and intensified density front. Based on these accumulation patterns, we identified six subregions in the PRE: UPPER, WEST, EAST, MO, HK, and SHELF. Across the subregions, there is a negative correlation between the net divergence ($\nabla_h \vec{V}_h$) and the accumulation probability, the intensified negative $\nabla_h \vec{V}_h$ provide the favorable conditions for water accumulation. The connections between the six subregions are discussed to illustrate the transport structure in the PRE. During summer, WEST and MO, with substantial net negative divergence and strong fronts, are powerful accumulation targets that attract particles from almost the entire estuary. The EAST and HK waters show a westward motion and are transported to the western estuary. In winter, the accumulated regions showed self-correlations, and particles were more likely to remain in the original regions. The UPPER becomes a major accumulation region owing to the blocking of the density front and the largely decreased river discharge. HK waters are transported to almost the entire estuary, contributing mainly to the accumulation in the WEST regions under westward currents. Sensitivity experiments were conducted to evaluate the effects of tidal currents and river discharge on accumulation patterns. Generally, tidal currents and river-induced gravitational circulation affect accumulation in different ways and affect different regions of the estuary. Their joint effects controlled the accumulation pattern. Tide currents promote accumulation in the WEST and UPPER regions during winter and in the MO and HK regions during summer through increased density stratification and changes in water column mixing (Fig. 15). Increased river discharge is conducive to seaside transport in the UPPER and WEST regions during summer and in the HK region during winter, which is related to the intensified offshore current and seaward movement of the density. With the removal of tidal currents and reduced river discharges, the intensified landward current and westward transport current from HK waters and the adjacent shelf will accelerate bottom-water intrusion from the lower estuary into the upper estuary.

4. Introduction: mass accumulation dynamics in different sub-regions in the PRE is an important part of the current study. If available, please supplement more previous findings on the different material accumulation features in these regions (e.g., total organic carbon, pollutants, suspended sediments, or other water quality parameter), to emphasize why we should care about dividing the PRE into the six subregions. Statements in lines 145-146 could fit in this part. It also needs to mention and explain why this study used a model producing climatological hydrodynamics rather than focusing on years

with realistic forcings.

Response: Thanks for the suggestions.

In the previous studies of accumulations in the PRE, D. Zhang et al. (2013) found trace elements had the highest concentration in the western part of PRE. The microplastics concentrated in Hong Kong water and western part of the PRE (Lam et al., 2020). Tao, Niu, Dong, Fu, and Lou (2021) revealed that accumulation of nitrogen and silicate appeared in the upper part of PRE and phosphorus pollution was observed in the northeast of PRE (e.g., Shenzhen Bay). Suspended solids are prone to gather in the head of the PRE in winter while the west part of the PRE in summer (X. Zhang et al., 2013). The total organic carbon is more likely to concentrate in Macau, Shenzhen Bay and Hong Kong (Guo, Ye, & Lian, 2016).

The six subregions were defined based on the accumulation regions obtained from the tracking (Figure 3b, d in the original manuscript). Those regions have different accumulation pattern and well fit the mass/pollutant accumulation regions in the previous studies, such as UPPER and WEST PRE are in accord with the accumulation of suspended solids and trace elements in X. Zhang et al. (2013) and D. Zhang et al. (2013).

Before reproducing the results in a specific year, we want to figure out the basic response of the accumulation dynamics under typical forcing and circulation in the PRE, and how it varies due to the changes in the tidal current and river discharge. Thus, in this study, the climatological forcing and hydrodynamics that could represent the typical seasonal feature were used to eliminate the possible anomalies caused by synoptic or interannual signals.

Following reviewer's suggestions, we integrate the above information in the revised manuscript:

Line 61-71:

With intensified human activities, pollutant sinks related to the accumulation phenomena in the PRE have attracted attention. Tao et al. (2021) revealed that the upper part of the PRE is a target sink for nitrogen and silicate. D. Zhang et al. (2013) found that trace elements prefer to accumulate on the PRE's west side. Higher concentrations of microplastics have been observed in western estuaries and Hong Kong waters (Lam et al., 2020). Similarly, studies on hypoxia have shown that the convergence of buoyancy-driven currents and wind-driven shelf flows contributes to the formation of stable water columns, providing favorable conditions for the development of hypoxic zones (e.g., D. Li et al. (2021); X. Li et al. (2020)). The high frequency of hypoxia in the estuary during summer is related to the strong stratification of the water column (Y. Cui, Wu, Ren, & Xu, 2019; H. Zhang & Li, 2010). These accumulation patterns in the PRE are more concerned with the measurement of pollutant concentrations (Tao et al., 2021), estimation of the pollutant accumulation rate (L. Zhang et al., 2009), and discussion of the sources of pollutants (Ye, Huang, Zhang, Tian, & Zeng, 2012), and lack a discussion on the understanding of accumulation spatial patterns and underlying physical control.

5. Line 13: 'plume fronts' only occurred in the abstract. Please use a consistent description on fronts with the main text.

   Response: Thanks a lot. The 'plume fronts' will be changed into 'river discharges' in the revised abstract. The description on the front is unified in the revised manuscript.

6. Line 65: is the right panel of Figure 1 the model domain? If so, clearly state it in the caption. If not,

please add a figure showing the model domain.

Response: Thanks for reviewer's reminder. The details of model domain have clearly shown in Figure R1. The regions inside the red line in Figure R1 are the model domain. The yellow line is the seaside boundary to identify whether the particles has left the estuary.

7. Line 77: climate → climatology. Which period did the climatology forcing represent for?

   Response: Thanks a lot. We will revise the typo. The climatology represents the mean forcing averaged between 1994 and 2018.

8. Lines 78-79: please supplement more detailed descriptions of the coarse resolution model or add related references.

   Response: Thanks for reviewer's reminder. There is a well validated coarser model simulates the shelf current which covers entire NSCS. The results provide the barotropic and baroclinic velocities, temperature, salinity, sea level along the boundaries of PRE. This model was well validated and used in previous investigations (L. Cui, Cai, & Liu, 2023; L. Cui et al., 2024; Deng et al., 2022).

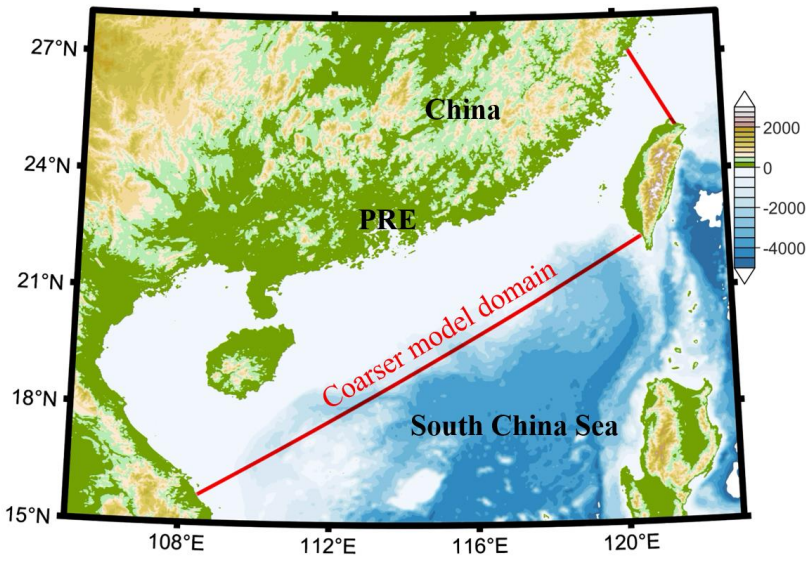

Figure R2. The domain of coarser model.

9. Line 79: clarify 'statistics of atmosphere forcing…'?
10. Line 80: what is the accuracy of the monthly river discharge rate by ECMWF in this region? Why not using the locally observed river discharge?

    Response: Thanks for reviews' reminder. Those two comments are related to the model configuration, we have responded in point 1 above. And the details can be found in Line 99-104 in the revised manuscript.

    Line 99-104: "Wind forcing, heat flux, and precipitation were obtained from ERA5 atmospheric reanalysis data from the European Center for Medium-Range Weather Forecasts (ECMWF) and were used to force ocean circulation through the implementation of the bulk computation algorithm (Fairall et al., 2003). The shelf current was obtained from a coarser model with good validation that can cover the North-South China Sea and provide information on the barotropic and baroclinic velocities, temperature, salinity, and sea level along the boundaries of the PRE (Deng et al., 2022)."

11. Line 87: what does ‘other complicated hydrodynamic processes’ imply? What is ‘computations’? Computations of particle trajectory? Also, please add references to support the statement: ‘The results of the computations…in the estuary-shelf system’.

Response: Thanks for the comment. The Lagrangian tracking model considers the advection, turbulence, individual behaviors of particles (e.g. vertical sinking, floating or swimming velocity), settlement and boundary behaviors during the particle trajectory simulations, which can support to obtain the approximate realistic trajectories in the real world with complicated hydrodynamic processes. The “computations” means the computation of the particle trajectories. This tracking module well captures the trajectories in previous studies (Chu et al., 2022a; Liang et al., 2021; North et al., 2011).

The sentences were refined to make it clear

Line 112-115: “To reasonably calculate the Lagrangian trajectories in the circulation of estuary-shelf systems, the tracking model considers the advection, turbulence, individual behaviors of particles (e.g., vertical sinking, floating, or swimming velocity), settlement, and boundary behaviors during particle trajectory simulations.”

Line 110-112: “Particle trajectories were traced by a three-dimensional offline Lagrangian TRANSport model (LTRANS v.2b), which captures complicated dynamical processes in the real world using Eulerian flow fields and turbulent mixing from the hydrodynamic model (Chu et al., 2022a; Liang et al., 2021; North et al., 2011).”

12. Line 90: clarify ‘different diffusivity coefficient’ in the vertical and horizontal turbulence.

Response: Thanks for the comment that helps us to correct the misleading in this sentence. The diffusivity coefficient is provided by the hydrodynamical model. In the hydrodynamical simulation, the vertical diffusivity was calculated through Mellor-Yamada 2.5 turbulence-closure module coefficient (Mellor & Yamada, 1982), which is widely used in the coastal simulation (Choi, Park, Choi, Jung, & Kim, 2021; J. Liu, Lu, & Li, 2019; Robertson & Hartlipp, 2017). While in horizontal direction, the harmonic horizontal diffusion with uniform value was used. The diffusive coefficient in output data was used by LTRANS to introduce the random walk during simulation.

We revised the manuscript to make it clear.

Line 106-108: “Vertical turbulence and diffusion coefficient are determined by the Mellor-Yamada 2.5 turbulence-closure module (Mellor & Yamada, 1982), which provides the turbulent mixing coefficient.”

13. Lines 91-93: the descriptions on particle tracking experiments are unclear. Were the 8386 particles released each day in January and July? How was the ‘uniform release’ achieved, i.e., what are the vertical and horizontal interval of each particle? How will the particle behave when they reach the boundaries, including open, land, surface, and bottom boundaries? time step of particle tracking? output frequency of the history files that were used to drive the particle tracking and the output frequency of particle location?

Response: Thanks for the comments.

For the surface tracking case, 8386 particles were released at the water surface, which are uniformly distributed covering the entire estuary and the adjacent shelf with a 0.01degree horizontal interval.

The particles were released every two days and tracked for 30 days after being released. The bottom tracking case is same as surface one but releasing at the bottom.

To drive the particle tracking in summer and winter, results from hydrodynamic simulation were saved each 20 minutes in January and July, respectively. During the tracking of trajectories, the time step of particle tracking is 30 seconds and the output frequency of the particles' location is 20 minutes. When particles reach the land, surface and bottom boundaries, it would be reflected back to the last step location and wait a suitable current to take it away. If they reach the boundaries of the model domain, the particles would only remain the last locations' information.

In the revised manuscript, we clarify the descriptions on the particle tracking experiments.

Line 122-126: "In the surface/bottom tracking case, 8386 particles were uniformly distributed at water surface/bottom across the estuary and adjacent shelf with a 0.01degree interval. Particles were released every two days and tracked for 30 days. The hydrodynamic simulation results were stored every 20 min in January and July to drive the particle tracking during summer and winter, respectively. During trajectory tracking, the time step of particle tracking was 30 seconds, and their locations were recorded every 20 minutes."

14. Line 105: it should be nit0

    Response: Corrected and thanks

15. Line 106: it is pt in equation (1). Please use the same symbol.

    Response: Thanks for reviewers' suggestion. The expression of the formula was carefully checked in the revised manuscript, and we will standardize the symbol in the formula.

16. Line 121: 'transport accumulation' seems to be an odd expression.

    Response: Thanks a lot. Actually, we want to express accumulation pattern here, perhaps our expression is not accurate. We will change it into 'Accumulation pattern and regional connectivity' in Line 150.

17. Lines 123-124: did particles come back after moving out of the seaside boundary?

    Response: When the particles move out of the seaside boundary of the estuary (the yellow line in Figure R1), it has the probability to return to the study area under the effect of tidal currents and wind forcing. If the particles reach the model domain, they will not come back again. We clarify this in the revised manuscript:

    Line 155-157: "If particles move beyond the seaside boundary of the estuary, they may return to the study area due to tidal currents and wind forcing. However, once the particles reached the model domain, they will not be backed again."

18. Line 135: particles were only tracked for 30 days as stated in section 2.1. Why would the maximum day in x-axis 60 days?

    Response: Thanks for reviewers' reminder. To choose a suitable time to explore the particle accumulation, we designed a test to get the trajectories for 60 days. As shown in Figure 2 in the manuscript, after 30 days, the most particles leave the estuary and the percentage decreased to less than 10%. Thus, in the following analysis, only the 30 days results were used to check the accumulation dynamics.

19. Line 148: What leads to the further landward intrusion of bottom water in winter?

Response: we select a typical transect in the PRE (Transect AB in Figure R4b) to show the changes of vertical structure of circulation. In winter, an obviously strengthened landward current is observed at the bottom, which is favorable for the bottom intrusion (Figure R3). The river discharge is larger in summer than that in winter in the PRE (Harrison, Yin, Lee, Gan, & Liu, 2008), and a strong outflow pushes the water to the lower estuary and hinders the intrusion of shelf water into the estuary. In winter, less river discharge leads to a weaker resistance to the intrusion water, which causes strengthened landward movement of the bottom water and pushes the isopycnals to move into the inner estuary. Thus, although the front is similar (Figure 6 in the original manuscript), the gravitational circulation induced by river discharge contributes to landward movement of water accumulation in winter.

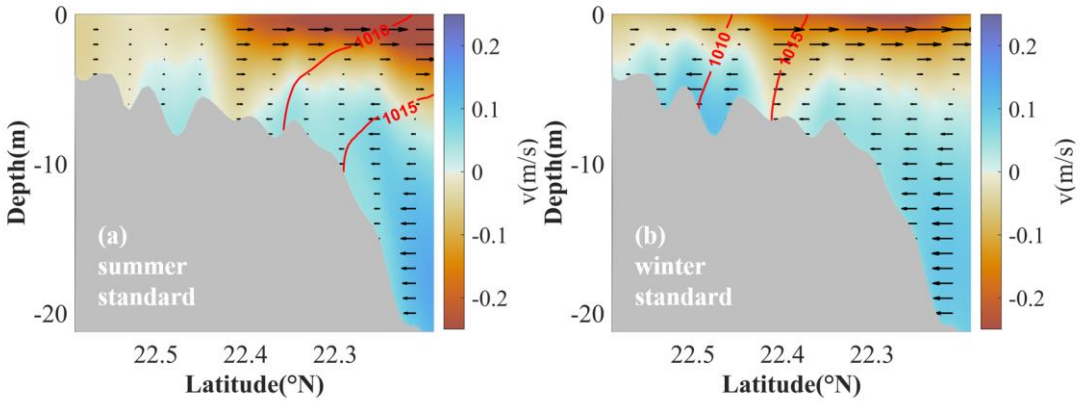

Figure R3. The flow field of standard in transect AB at the bottom layer in summer (a) and winter (b), respectively. The colorbar represents the onshore velocity, the positive value means the landward motion in the transect AB. The arrow represents the current direction and the length is the strength of currents. The red line represents the isopycnal of 1010 kg/m^{-3} and 1015 kg/m^{-3}.

20. Line 155. Does probability have a unit? percentage? It is not easy to see the difference in the gray color for velocity arrows. Suggest using arrow length to represent the magnitude of velocity. In addition, there are some unnecessary gray dividing lines in Figure 3 and figures below. Please remove them.

Response: Thanks for reviewers' reminder. The accumulation probability is calculated based on the percentage and does not have a unit.

The flow field will be separated from Figure 3 in the original manuscript and show below, and a more obvious colormap will be used to represent the velocity changes in the new version of flow field. The gray dividing lines in Figure 3 in the original manuscript will also be removed.

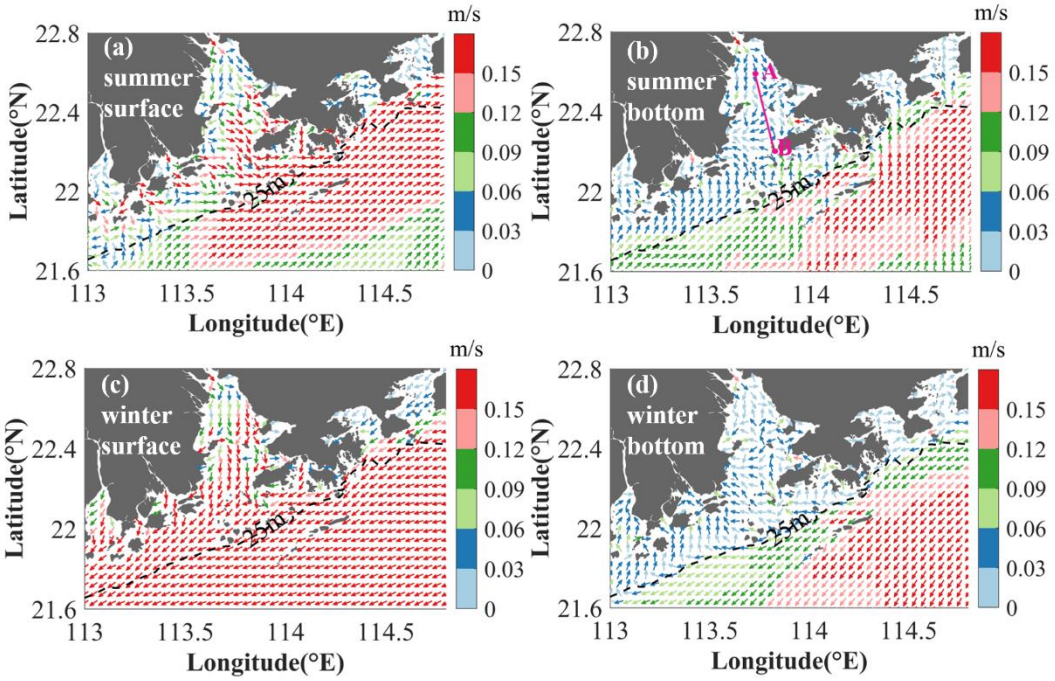

Figure R4. The flow field at the surface layer (a) and bottom layer (b) during summer time. (c-d) are same as (a-b), except for during winter time. The colorbar represents the velocity of current.

21. Line 182: the accumulation probability was averaged over each sub-domain and not differentiate between surface and bottom in Figure 5? The div(V) in Figure 5c-d shows surface or bottom or depth-averaged results?

Response: Thanks for reviewers' comments. The accumulation probability in Figure 5 in original manuscript is averaged in bottom of each subregion. As shown in Figure R5, the bottom has a much larger accumulation, while the surface features with the strong offshore transport, as Lam et al. (2020) founded higher concentration of microplastics at the bottom layer than at the surface layer in the PRE. Therefore, we chose the bottom layer to discuss the internal connection and accumulation dynamics between different regions in the PRE. The accumulation and DIV were calculated at the bottom layer. We clarify this in the manuscript:

Line 227-230: "The bottom divergence of the horizontal current, i.e., $\nabla_h \vec{V}_h = \frac{\partial u}{\partial x} + \frac{\partial v}{\partial y}$, which u and v represent the bottom zonal and meridional velocity, is calculated to examine its influence on the identified bottom accumulation regions (Fig. 7a, b). We established a connection between the average accumulation probability in each subregion and the divergence of the horizontal current."

Line 239-240: "Spatial distribution of $\nabla_h \vec{V}_h$ also illustrates that the intensified negative values occur in the region of the high accumulation probability (Fig. 7c-d)"

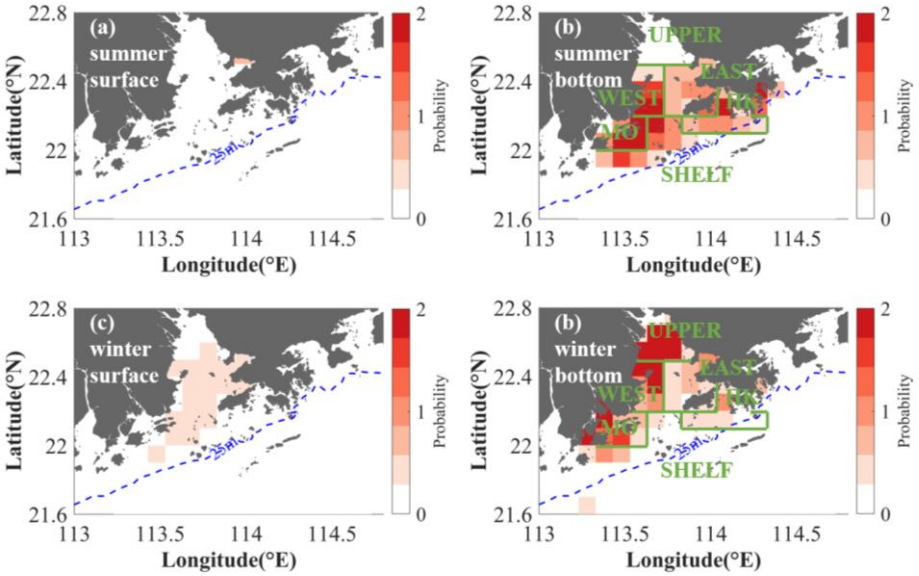

Figure R5: (a–b) Accumulation probability (color, D^{t_0} in Eq. (2)) at the surface layer and bottom layer during summer time, respectively. The color bar indicates the magnitude of the accumulation probability. (c-d) is the same as (a-b) but winter time.

22. Line 215: the unit of density front should be kg m-4 from the equation in line 205.

Response: Thanks for reviewers' kindly reminder, we corrected the typo in the revised manuscript.

23. Section 3.3: please provide more details on the testing cases (or put them in the supplementary). For example, which options or files in roms were removed for the case removing tidal currents. How many rivers were included in the model domain? A time series of river discharge in base case and test case will be useful information.

Response: Thanks for reviewers' suggestions.

In the ROMs, the wind forcing, river discharge and tidal current were provided by different forcing files. The model read those forcing files during the simulation. In the sensitivity test, the configuration was the same but the magnitude of the wind speed, river discharge rate and tidal current were changed respectively. In the sensitivity case with reduced river discharges, the magnitude of river discharge rate is decreased to 20% of the control run. In the no tide case, the tide induced current and elevation is not included along the open boundary conditions.

To make the configuration of the model clear, we added the supplementary file to introduce the monthly river discharges and seasonal monsoon (Figure R6). The configuration of the sensitivity test was also clarified in the revised manuscript.

Line 269-271: "In the case of reduced river discharge, the magnitude of river discharge in the forcing file was reduced by 20%. The magnitude of the tidal current was set to zero to remove the tidal currents."

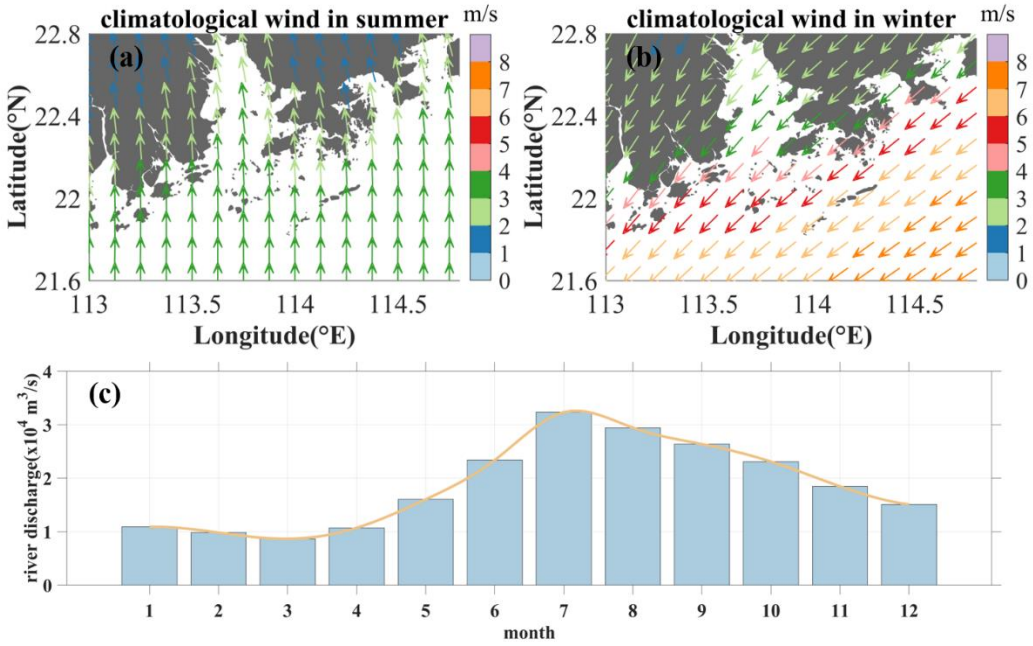

Figure R6. (a-b) The seasonal mean wind speed (m/s) during summer (June–August) and winter (December–February), respectively. (c) The monthly river discharge in the PRE.

24. Line 244: if the particle tracking was conducted for a longer time, will MO accumulate water from other regions?

Response: Thanks a lot. Since the particles will finally leave the estuary (Figure 2 in the original manuscript), the longer tracking time does not make MO accumulate water from other regions. We have a test with a longer tracking period of 30 days, the basic accumulation pattern and the connection among the different regions are similar.

25. Line 245: the arrows in Figure 7c-d seems to be confusing. Not every regions were noted by arrows? What does different arrow directions represent?

Response: Thanks for reviewers' reminder. We only choose the region with a larger accumulation anomaly to plot the arrows in the figure. The direction of the figure represents the changes of the accumulation and divergence in each sensitivity test. Generally, in those cases we noticed a clear negative relationship between the accumulation and divergence. For example, in the no tide case during summer time (Figure R7), the left-upward arrow of the EAST point represents the strengthened of net convergence (leftward) and increased accumulation (upward).

In the revised manuscript we make it clear that the arrows are plotted mainly in the regions with significant accumulation changes.

Line 302-304: "The arrow represents the changes of $\nabla_h \vec{V}_h$ and accumulation due to the removal of tidal currents in the region, with significant changes in the accumulation."

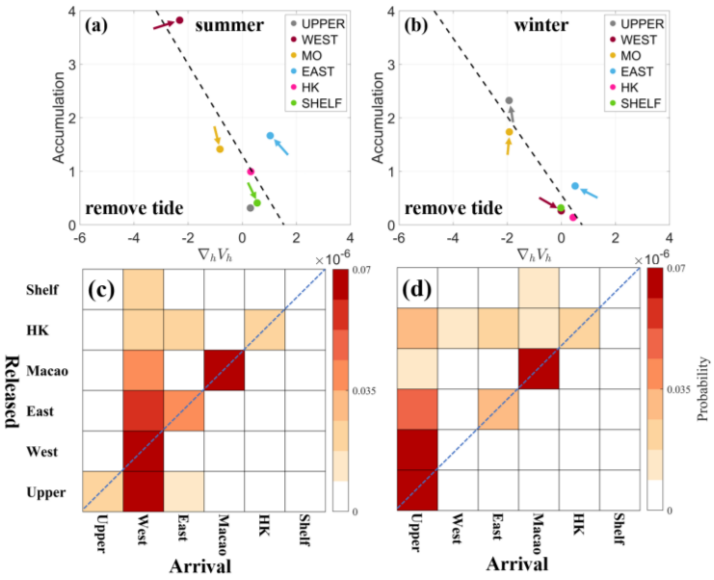

Figure R7: (a-b) Scatter plot of accumulation probability against $\nabla_h \vec{V}_h$ for various subregions during summer and winter in removing tide cases. The arrow represents the changes of $\nabla_h \vec{V}_h$ and accumulation due to the removing of tide in each subregion. (c-d) The connection between six regions for removal of tidal current at the bottom layer during summer and winter time, respectively.

26. Line 281: suggest adding some descriptions on wind strength and magnitude of river discharge in the main text.

Response: Thanks a lot. According to reviewers' comments, some basic information of wind forcing and river discharge in the PRE are supplemented in Line26-47 in the revised manuscript, which can provide a better background of the PRE.

Line 26-47:

The Pearl River Estuary (PRE), located in the northern South China Sea (NSCS) (Fig. 1a), is influenced by the East Asian Monsoon, with northeasterly winds prevailing in winter and southwesterly winds prevailing in summer (T. Li & Li, 2018). Thus, in the PRE, winter is characterized as a dry season, and summer is characterized as a wet season due to the large rainfall induced by the moist air brought from the South China Sea; consequently, the river discharge in summer (~ 20,000 m^3s^{-1}) is approximately five times more than that in winter (~ 3,600 m^3s^{-1}) (Harrison et al., 2008). This is quite different from many other river deltas, such as the Mississippi deltas, where river discharge reaches a maximum in winter and spring, but is reduced in summer and autumn (Lane et al., 2007).

As a bell-shaped estuary, the width increases from approximately 5 km at the upper end to 35 km at the lower end. Despite the two narrow, deeper channels (~20 m in depth), the PRE is shallow, with a water depth of approximately 2-10 m. The PRE is a partially mixed estuary in which circulation is jointly controlled by river discharge, tides, wind, and topography (Ascione Kenov, Garcia, & Neves, 2012; Banas & Hickey, 2005; Gong, Shen, & Hong, 2009; He, Yin, Stocchino, & Wai, 2023; He, Yin, Stocchino, Wai, & Li, 2022; Z. Liu, Zu, & Gan, 2020). There are two distinct dynamic regimes in the PRE. The narrow upper part of the PRE shows classical gravitational circulation, whereas in the wider lower part of the PRE, where the Coriolis effect becomes essential, the topography and interaction with the monsoon-driven shelf current complicate the circulation (Dong, Su, Ah Wong, Cao, & Chen,

2004; Wong et al., 2003; Zu & Gan, 2015). Gravitational circulation occurs in the two deep channel regions, whereas currents show precise seasonal characteristics over the shallower western estuary. Geostrophic wind-driven coastal currents intrude into the PRE during the summer upwelling season (Zu & Gan, 2015), whereas seaward buoyancy-driven coastal currents flow out of the PRE during winter(Dong et al., 2004; Wong et al., 2003). The alternation of the spring-neap tide and variation in river discharge play crucial roles in modulating stratification and mixing inside the PRE (Mao, Shi, Yin, Gan, & Qi, 2004; Pan, Lai, & Thomas Devlin, 2020; Zu, Wang, Gan, & Guan, 2014). Strong tidal mixing in the middle PRE has led to the conversion of estuarine river plumes into buoyancy-driven coastal currents (Dong et al., 2004; Zu et al., 2014).

Technical corrections:

1. Line 13: add 'of particles' or other appropriate words after 'bottom-layer accumulations'.

Response: added and thanks.

2. Line 15: add 'a' after 'there is'

Response: added and thanks.

3. Line 16: local → locally

Response: corrected.

4. Line 30: add 'the' after 'Located in'

Response: added and thanks.

5. Line 35: change 'Such as' to 'For example,'

Response: corrected.

6. Line 43: were → are

Response: corrected.

7. Line 46: stronger → strong

Response: corrected.

8. Line 51: remained → remain

Response: corrected.

9. Line 60: explored → explore

Response: corrected.

10. Line 159: subdivide → divide

Response: corrected.

11. Line 164: where → which

Response: corrected.

12. Line 203: accumulating → accumulate; add 'the' between 'in middle'

Response: corrected and added. Thanks.

13. Line 219: contribution → contributions

Response: corrected.

Reference:

Ascione Kenov, I., Garcia, A. C., & Neves, R. (2012). Residence time of water in the Mondego estuary (Portugal). *Estuarine, coastal and shelf science, 106*, 13-22. doi:10.1016/j.ecss.2012.04.008

Banas, N. S., & Hickey, B. M. (2005). Mapping exchange and residence time in a model of Willapa Bay, Washington, a branching, macrotidal estuary. *Journal of Geophysical Research, 110*(C11), C11011-n/a. doi:10.1029/2005JC002950

Cai, Z., Liu, G., Liu, Z., & Gan, J. (2022). Spatiotemporal variability of water exchanges in the Pearl River Estuary by interactive multiscale currents. *Estuarine, coastal and shelf science, 265*, 107730. doi:10.1016/j.ecss.2021.107730

Choi, Y., Park, Y., Choi, M., Jung, K. T., & Kim, K. O. (2021). A Fine Grid Tide-Wave-Ocean Circulation Coupled Model for the Yellow Sea: Comparison of Turbulence Closure Schemes in Reproducing Temperature Distributions. *Journal of Marine Science and Engineering, 9*(12), 1460. Retrieved from https://www.mdpi.com/2077-1312/9/12/1460

Chu, N., Liu, G., Xu, J., Yao, P., Du, Y., Liu, Z., & Cai, Z. (2022a). Hydrodynamical transport structure and lagrangian connectivity of circulations in the Pearl River Estuary. *9*. doi:10.3389/fmars.2022.996551

Chu, N., Liu, G., Xu, J., Yao, P., Du, Y., Liu, Z., & Cai, Z. (2022b). Hydrodynamical transport structure and lagrangian connectivity of circulations in the Pearl River Estuary. *Frontiers in Marine Science, 9*. doi:10.3389/fmars.2022.996551

Cui, L., Cai, Z., & Liu, Z. (2023). Water exchange and transport pathways in estuary-shelf region of Pearl River Estuary under multiple forcings. *Continental shelf research, 266*, 105099. doi:10.1016/j.csr.2023.105099

Cui, L., Liu, Z., Chen, Y., & Cai, Z. (2024). Three-Dimensional Water Exchanges in the Shelf Circulation System of the Northern South China Sea Under Climatic Modulation From ENSO. *Journal of Geophysical Research: Oceans, 129*(4), e2023JC020290. doi:https://doi.org/10.1029/2023JC020290

Cui, Y., Wu, J., Ren, J., & Xu, J. (2019). Physical dynamics structures and oxygen budget of summer hypoxia in the Pearl River Estuary. *Limnology and Oceanography, 64*(1), 131-148. doi:https://doi.org/10.1002/lno.11025

Deng, Y., Liu, Z., Zu, T., Hu, J., Gan, J., Lin, Y., . . . Cai, Z. (2022). Climatic Controls on the Interannual Variability of Shelf Circulation in the Northern South China Sea. *Journal of Geophysical Research: Oceans, 127*(7), e2022JC018419. doi:https://doi.org/10.1029/2022JC018419

Dong, L., Su, J., Ah Wong, L., Cao, Z., & Chen, J.-C. (2004). Seasonal variation and dynamics of the Pearl River plume. *Continental shelf research, 24*(16), 1761-1777. doi:10.1016/j.csr.2004.06.006

Fairall, C. W., Bradley, E. F., Hare, J., Grachev, A. A., & Edson, J. B. (2003). Bulk parameterization of air–sea fluxes: Updates and verification for the COARE algorithm. *Journal of climate, 16*(4), 571-591.

Gong, W., Shen, J., & Hong, B. (2009). The influence of wind on the water age in the tidal Rappahannock River. *Marine Environmental Research, 68*(4), 203-216. doi:https://doi.org/10.1016/j.marenvres.2009.06.008

Guo, W., Ye, F., & Lian, Z. (2016). Seasonal changes of organic carbon in the Pearl River estuary. *Re dai hai yang xue bao, 35*(4), 40-50.

Harrison, P. J., Yin, K., Lee, J. H. W., Gan, J., & Liu, H. (2008). Physical–biological coupling in the Pearl River Estuary. *Continental shelf research, 28*(12), 1405-1415. doi:https://doi.org/10.1016/j.csr.2007.02.011

He, C., Yin, Z.-Y., Stocchino, A., & Wai, O. W. H. (2023). Generation of macro-vortices in estuarine compound channels. *Frontiers in Marine Science, 10*. doi:10.3389/fmars.2023.1082506

He, C., Yin, Z.-Y., Stocchino, A., Wai, O. W. H., & Li, S. (2022). The coastal macro-vortices dynamics in Hong Kong waters and its impact on water quality. *Ocean Modelling, 175*, 102034.

doi:https://doi.org/10.1016/j.ocemod.2022.102034

Lam, T. W. L., Fok, L., Lin, L., Xie, Q., Li, H.-X., Xu, X.-R., & Yeung, L. C. (2020). Spatial variation of floatable plastic debris and microplastics in the Pearl River Estuary, South China. *Marine pollution bulletin, 158*, 111383. doi:https://doi.org/10.1016/j.marpolbul.2020.111383

Lane, R. R., Day, J. W., Marx, B. D., Reyes, E., Hyfield, E., & Day, J. N. (2007). The effects of riverine discharge on temperature, salinity, suspended sediment and chlorophyll a in a Mississippi delta estuary measured using a flow-through system. *Estuarine, coastal and shelf science, 74*(1), 145-154. doi:https://doi.org/10.1016/j.ecss.2007.04.008

Li, D., Gan, J., Hui, C., Yu, L., Liu, Z., Lu, Z., . . . Dai, M. (2021). Spatiotemporal Development and Dissipation of Hypoxia Induced by Variable Wind-Driven Shelf Circulation off the Pearl River Estuary: Observational and Modeling Studies. *126*(2), e2020JC016700. doi:https://doi.org/10.1029/2020JC016700

Li, T., & Li, T.-J. (2018). Sediment transport processes in the Pearl River Estuary as revealed by grain-size end-member modeling and sediment trend analysis. *Geo-Marine Letters, 38*(2), 167-178. doi:10.1007/s00367-017-0518-2

Li, X., Lu, C., Zhang, Y., Zhao, H., Wang, J., Liu, H., & Yin, K. (2020). Low dissolved oxygen in the Pearl River estuary in summer: Long-term spatio-temporal patterns, trends, and regulating factors. *Marine pollution bulletin, 151*, 110814-110814. doi:10.1016/j.marpolbul.2019.110814

Liang, J.-H., Liu, J., Benfield, M., Justic, D., Holstein, D., Liu, B., . . . Dong, W. (2021). Including the effects of subsurface currents on buoyant particles in Lagrangian particle tracking models: Model development and its application to the study of riverborne plastics over the Louisiana/Texas shelf. *Ocean modelling (Oxford), 167*, 101879. doi:10.1016/j.ocemod.2021.101879

Liu, J., Lu, S., & Li, Y. (2019). Numerical study on sensibility of turbulence closure schemes at Oujiang River Estuary. *Applied Ocean Research, 88*, 76-88. doi:https://doi.org/10.1016/j.apor.2019.04.014

Liu, Z., Zu, T., & Gan, J. (2020). Dynamics of cross-shelf water exchanges off Pearl River Estuary in summer. *Progress in Oceanography, 189*, 102465. doi:https://doi.org/10.1016/j.pocean.2020.102465

Mao, Q., Shi, P., Yin, K., Gan, J., & Qi, Y. (2004). Tides and tidal currents in the Pearl River Estuary. *Continental shelf research, 24*(16), 1797-1808. doi:10.1016/j.csr.2004.06.008

Mellor, G. L., & Yamada, T. (1982). Development of a turbulence closure model for geophysical fluid problems. *Reviews of Geophysics, 20*(4), 851-875. doi:https://doi.org/10.1029/RG020i004p00851

North, E. W., Adams, E. E. E., Schlag, Z. Z., Sherwood, C. R., He, R. R., Hyun, K. H. K., . . . Enterprise, M. t. D. H. O. S. A. R. B. (2011). Simulating oil droplet dispersal from the Deepwater Horizon spill with a Lagrangian approach. *195*, 217-226.

Pan, J., Lai, W., & Thomas Devlin, A. (2020). Circulations in the Pearl River Estuary: Observation and Modeling. In *Estuaries and Coastal Zones - Dynamics and Response to Environmental Changes*.

Robertson, R., & Hartlipp, P. (2017). Surface wind mixing in the Regional Ocean Modeling System (ROMS). *Geoscience Letters, 4*(1), 24. doi:10.1186/s40562-017-0090-7

Shchepetkin, A. F., & McWilliams, J. C. (2005). The regional oceanic modeling system (ROMS): a split-explicit, free-surface, topography-following-coordinate oceanic model. *Ocean modelling (Oxford), 9*(4), 347-404. doi:10.1016/j.ocemod.2004.08.002

Song, Y., & Haidvogel, D. (1994). A Semi-implicit Ocean Circulation Model Using a Generalized Topography-Following Coordinate System. *Journal of Computational Physics, 115*(1), 228-244. doi:https://doi.org/10.1006/jcph.1994.1189

Tao, W., Niu, L., Dong, Y., Fu, T., & Lou, Q. (2021). Nutrient Pollution and Its Dynamic Source-Sink Pattern in the Pearl River Estuary (South China). *Frontiers in Marine Science, 8*. doi:10.3389/fmars.2021.713907

Wong, L. A., Chen, J. C., Xue, H., Dong, L. X., Su, J. L., & Heinke, G. (2003). A model study of the circulation in the Pearl River Estuary (PRE) and its adjacent coastal waters: 1. Simulations and comparison with observations. *Journal of Geophysical Research: Oceans, 108*(C5). doi:https://doi.org/10.1029/2002JC001451

Ye, F., Huang, X., Zhang, D., Tian, L., & Zeng, Y. (2012). Distribution of heavy metals in sediments of the Pearl River Estuary, Southern China: Implications for sources and historical changes. *Journal of Environmental Sciences, 24*(4), 579-588. doi:https://doi.org/10.1016/S1001-0742(11)60783-3

Zhang, D., Zhang, X., Tian, L., Ye, F., Huang, X., Zeng, Y., & Fan, M. (2013). Seasonal and spatial dynamics of trace elements in water and sediment from Pearl River Estuary, South China. *Environmental Earth Sciences, 68*(4), 1053-1063. doi:10.1007/s12665-012-1807-8

Zhang, H., & Li, S. (2010). Effects of physical and biochemical processes on the dissolved oxygen budget for the Pearl River Estuary during summer. *Journal of marine systems, 79*(1), 65-88. doi:https://doi.org/10.1016/j.jmarsys.2009.07.002

Zhang, L., Yin, K., Wang, L., Chen, F., Zhang, D., & Yang, Y. (2009). The sources and accumulation rate of sedimentary organic matter in the Pearl River Estuary and adjacent coastal area, Southern China. *Estuarine, coastal and shelf science, 85*(2), 190-196. doi:https://doi.org/10.1016/j.ecss.2009.07.035

Zhang, X., Shi, Z., Liu, Q., Ye, F., Tian, L., & Huang, X. (2013). Spatial and temporal variations of picoplankton in three contrasting periods in the Pearl River Estuary, South China. *Continental shelf research, 56*, 1-12. doi:https://doi.org/10.1016/j.csr.2013.01.015

Zu, T., & Gan, J. (2015). A numerical study of coupled estuary–shelf circulation around the Pearl River Estuary during summer: Responses to variable winds, tides and river discharge. *Deep Sea Research Part II: Topical Studies in Oceanography, 117*, 53-64. doi:https://doi.org/10.1016/j.dsr2.2013.12.010

Zu, T., Gan, J., & Erofeeva, S. Y. (2008). Numerical study of the tide and tidal dynamics in the South China Sea. *Deep Sea Research Part I: Oceanographic Research Papers, 55*(2), 137-154. doi:https://doi.org/10.1016/j.dsr.2007.10.007

Zu, T., Wang, D., Gan, J., & Guan, W. (2014). On the role of wind and tide in generating variability of Pearl River plume during summer in a coupled wide estuary and shelf system. *Journal of marine systems, 136*, 65-79. doi:https://doi.org/10.1016/j.jmarsys.2014.03.005